Glucose influences endometrial receptivity to embryo implantation through O-GlcNAcylation-mediated regulation of the cytoskeleton

Peter T Ruane[1,2], Isabel Paterson[1,2], Beth Reeves[1,2], Daman Adlam[1,2], Stéphane C Berneau[1,2], Lewis Renshall[1,2], Jan J Brosens[3], Susan J Kimber[4], Daniel R Brison[1,5], John D Aplin[1,2] and Melissa Westwood[1,2]

[1]Maternal and Fetal Health Research Centre, Division of Developmental Biology and Medicine, School of Medical Sciences, Faculty of Biology, Medicine and Health, University of Manchester, St. Mary's Hospital, Manchester, UK, M13 9WL

[2]Manchester University NHS Foundation Trust, Manchester Academic Health Sciences Centre, Manchester, UK, M13 9WL

[3]Obstetrics and Gynaecology, Division of Biomedical Sciences, Clinical Sciences Research Laboratory, Warwick Medical School, Warwick, Coventry, UK

[4]Division of Cell Matrix Biology and Regenerative Medicine, School of Biological Sciences, Faculty of Biology Medicine and Health, University of Manchester, Michael Smith Building, Manchester, UK, M13 9PT

[5]Department of Reproductive Medicine, Old St. Mary's Hospital, Manchester University NHS Foundation Trust, Manchester Academic Health Science Centre, Oxford Road, Manchester, UK, M13 9WL

Running Head

Glucose-regulated mechanisms in embryo implantation

Corresponding Author: Melissa Westwood, Maternal and Fetal Health Research Centre, University of Manchester. Tel: +44(0)161 276 5461; melissa.westwood@manchester.ac.uk

Abstract

Phenotypic changes to endometrial epithelial cells underpin receptivity to embryo implantation at the onset of pregnancy but the effect of hyperglycaemia on these processes remains poorly understood. Here we show that physiological levels of glucose (5mM) abolished receptivity in the endometrial epithelial cell line, Ishikawa. However, embryo attachment was supported by 17mM glucose as a result of glucose flux through the hexosamine biosynthetic pathway (HBP) and modulation of cell function via protein O-GlcNAcylation. Pharmacological inhibition of HBP or protein O-GlcNAcylation reduced embryo attachment in co-cultures at 17mM glucose. Mass spectrometry analysis of the O-GlcNAcylated proteome in Ishikawa cells revealed that myosin phosphatase target subunit 1 (MYPT1) is more highly O-GlcNAcylated in 17mM glucose, correlating with loss of its target protein, phospho-myosin light chain 2, from apical cell junctions of polarised epithelium. 2D and 3D morphologic analysis demonstrated that the higher glucose level attenuates epithelial polarity through O-GlcNAcylation. Inhibition of RhoA-associated kinase (ROCK) or myosin II led to reduced polarity and enhanced receptivity in cells cultured in 5mM glucose, consistent with data showing that MYPT1 acts downstream of ROCK signalling.

These data implicate regulation of endometrial epithelial polarity through RhoA signaling upstream of actomyosin contractility in the acquisition of endometrial receptivity. Glucose levels impinge on this pathway through O-GlcNAcylation of MYPT1, which may impact endometrial receptivity to an implanting embryo in women with diabetes.

New & Noteworthy

Understanding how glucose regulates endometrial function will support pre-conception guidance and/or the development of targeted interventions for individuals living with diabetes wishing to embark on pregnancy. We found that glucose can influence endometrial epithelial cell receptivity to embryo implantation by regulating post-translational modification of proteins involved in the maintenance of cell polarity. Impaired or inappropriate endometrial receptivity could contribute to fertility and/or early pregnancy complication caused by poor glucose control.

Key Words

Implantation; pregnancy; polarity; post-translational modification; diabetes

Introduction

The rising prevalence of both type 1 and type 2 diabetes means that by the end of this decade, 90 million women of reproductive age will be affected by diabetes (1) and the attendant risk of infertility (2) or poor pregnancy outcomes (3, 4). Despite improvements in clinical management, only a minority of women with type 1 (16%) or type 2 (38%) diabetes achieve the internationally agreed (5) target of <6.5% glycated haemoglobin around the time of conception (6). Furthermore, even apparently well-controlled subjects can have high post-prandial spikes of plasma glucose (7). The concentration of glucose in uterine fluid reflects that of the circulation (8); thus the endometrium of women with diabetes will be exposed to intermittently (post-prandial) or chronically high levels of glucose, depending on the individual's level of control. Animal studies suggest that high glucose levels are detrimental to endometrial function (9, 10).

At implantation, attachment of the blastocyst-stage embryo to the uterine luminal epithelium is followed by invasion of underlying endometrial stroma and access to the maternal vasculature. Attachment occurs 7-8 days after the pre-ovulatory surge in luteinising hormone, when endocrine signalling from the corpus luteum and paracrine signalling from the stroma have promoted a receptive luminal epithelial phenotype (11), including modification of the glycocalyx, expression of adhesion molecules, and a reduction in epithelial cell polarity mediated by re-modelling of junctional complexes (12). Impaired receptivity leading to problems in implantation is a major cause of reduced fecundity (13) and miscarriage during the first trimester (14).

Data from studies of human assisted reproduction show that receptivity is maternally controlled (15), however little is known about the molecular mechanisms that translate abnormal glucose availability into altered endometrial behaviour. In other tissues, the hexosamine biosynthetic pathway (HBP) is a nutrient-driven regulator of cellular function (16) including aspects of epithelial polarity (11). HBP activation results in the synthesis of uridine diphosphate N-acetyl glucosamine (UDP-GlcNAc), which is used to glycosylate proteins post-translationally. O-GlcNAcylation at serine or threonine residues is catalysed by O-GlcNAc transferase (OGT), which targets a functionally-diverse range of nucleocytoplasmic proteins to regulate their degradation, location, interaction with binding partners and potential to be phosphorylated by kinases (16). O-GlcNAcase (OGA) is responsible for removing the GlcNAc moieties.

Cells use the HBP to sense both low and high glucose concentrations, although the resultant profile of GlcNAcylated proteins differs between the two conditions as the substrate specificities of OGT depend on UDP-GlcNAc concentration (17). Consequently, altered

protein O-GlcNAcylation is evident in the blood cells of individuals with diabetes (18, 19). Moreover, altered O-GlcNAcylation might influence endometrial function. Mice treated with glucosamine, which enters the HBP downstream of the rate-limiting enzyme glutamine-fructose-6-phosphate transaminase 1 (GFPT1), have reduced litter size (20) and in animals with streptozotocin-induced diabetes, the overall level of O-GlcNAcylated proteins is increased in uterine luminal epithelium and the number of viable implantation sites is reduced (21).

Here we used an *in vitro* model of implantation to investigate the impact of glucose-induced changes in endometrial protein O-GlcNAcylation on receptivity. Our data show that enhanced glucose flux through the HBP is associated with increased receptivity, likely due to a reduction in epithelial polarity caused by modulation of apical junctional function by O-GlcNAcylation of proteins in the ras homologous (Rho) / Rho-associated protein kinase (ROCK) / myosin light chain (MLC) signalling pathway.

Research Design and Methods

Mouse Embryos: Two-cell mouse embryos were obtained from eight-week old female CD-1 mice in accordance with our Home Office licence under the Animal Act, 1986 and local ethical approval of our protocol (22). Embryos were matured to embryonic day (E)4.5 blastocysts *ex vivo* (3 days in potassium simplex optimised medium containing 2mM glucose + 0.4% BSA, 5% CO_2, 37ºC), hatched from the zona pellucida using acid Tyrode's (pH 2.5). Hatched E4.5 blastocysts were either added into co-culture with Ishikawa cells or cultured in 1:1 DMEM:F12 containing 17mM glucose + 0.4% BSA for a further 24h, to E5.5, depending on experimental requirements.

Ishikawa cell culture and embryo attachment assay: Ishikawa cells (ECACC 99040201) were maintained in 1:1 DMEM:F12 medium containing either 5mM or 17mM glucose and supplemented with 10% FCS, 2mM L-glutamine, 100µg/ml streptomycin and 100IU/ml penicillin. Cells to be used for embryo attachment experiments were seeded in medium containing 5mM or 17mM glucose alongside individual inhibitors as per experimental treatment group: 100µM 6-diazo-5-oxo-L-norleucine (DON; Sigma), an inhibitor of GFPT1; 10µM OSMI1 (Sigma), which inhibits OGT; 5µM Thiamet-g (Sigma), which inhibits OGA; 1µM Blebbistatin (Sigma) or 10µM Y27632 (Sigma), inhibitors of Myosin II and ROCK, respectively. Then, twenty four hours prior to adding embryos to the cultures, cells were switched to serum-free DMEM:F12, containing experiment-appropriate glucose levels and inhibitors.

Just before starting the attachment assay, inhibitors were removed (to ensure that any effect on attachment was due to changes in endometrial rather than embryo function) by re-plenishing cultures with serum-free medium then three E5.5 blastocysts per well were added and the cultures continued for a further 24h, to E6.5. Stability of embryo attachment was determined by observation under an inverted phase contrast microscope (Evos XL Core) at 4, 8, 12 and 24 hours of co-culture using a 4-point scale based on blastocyst movement following sample agitation as shown in the Movie in (22). In some experiments, E4.5 blastocysts were co-cultured in suspension above Ishikawa cells in transwells with 8µm pores (Corning).

Data were statistically analysed using Prism software (Graph-Pad, USA) and the two-way ANOVA test followed by Bonferroni's multiple comparisons post-hoc test, and are shown as mean (±SEM) percentage of stably attached blastocysts.

Quantitative PCR (qPCR) analysis of trophoblast gene expression: E4.5 blastocysts were cultured alone or co-cultured with Ishikawa cells in 1:1 DMEM:F12 containing 5mM or 17mM glucose, for 24h. As E5.5 blastocysts do not attach stably, they were released from the coculture by gentle pipetting then lysed for RNA extraction (10 blastocysts per condition) using the RNeasy Micro kit (Qiagen, Manchester, UK). The RNA was reverse transcribed using random 9mer primers (Agilent, Wokingham, UK) and a Sensiscript RT kit (Qiagen). qPCR analysis to assess the expression of *Hand1* and *Eomes* was performed as previously described (23). Fold change in expression was calculated using the 2-ΔΔct method and differences were assessed using Mann-Whitney tests.

Mass spectroscopy analysis of the Ishikawa cell proteome and O-GlcNAcome: Ishikawa cells grown in medium containing either 5mM glucose, 17mM glucose or 17mM glucose + 10µM OSMI1 were lysed in radioimmunoprecipiation assay (RIPA) buffer containing protease inhibitors and 5µM Thiamet-g (Sigma, an inhibitor of OGA) then 25µg protein from each sample was removed for mass spectroscopy of the full proteome and 250µg protein was pre-cleared using plain agarose beads (1h at 4°C) to remove non-specifically bound protein, then incubated with beads conjugated with succinylated wheat germ agglutinin (sWGA; Sigma UK), which recognises GlcNAc, overnight at 4°C to generate samples for analysis of the O-GlcNAcome. Samples were prepared for liquid chromatography coupled-mass spectrometry/mass spectrometry (LC-MS/MS) as previously described (24) then analysed using an UltiMate® 3000 Rapid Separation LC (Dionex Corporation, USA) coupled to an Orbitrap Elite (Thermo Fisher Scientific, USA) mass spectrometer. Peptide mixtures were separated for 44 min at 300nl/min-1 using a 1.7µM

Ethylene Bridged Hybrid C18 analytical column (75 mm x 250µm internal diameter; Waters, USA) and 0.1% formic acid in a gradient of 8-33% acetonitrile.

The identified peptides were mapped using Mascot 2.5.1 (Matrix Science UK), to the *Homo Sapiens* proteome. Mascot 2.5.1 was used with a fragment tolerance of 0.60 Da (Monoisotopic), a parent tolerance of 5.0 parts per million (Monoisotopic), fixed modifications of +57 on C (Carbamidomethyl), variable modifications of +16 on M (Oxidation). A maximum of 1 missed cleavage was permitted. .DAT files from Mascot were analysed using Scaffold (Proteome Software, USA), employing the following thresholds: 95% protein identification certainty, 1 for the minimum number of unique peptides mapping to each protein, and 80% peptide identification certainty. Proteins were quantified according to the normalised spectral abundance factor (NSAF) and differential abundance between 5mM glucose, 17mM glucose or 17mM glucose + 10µM OSMI1 was calculated and compared using a t-test.

Bioinformatic analysis: Hierarchical clustering analysis was performed on differentially enriched proteins in the O-GlcNAcome using ClustVis. Mapped O-GlcNAc sites in proteins were identified using the O-GlcNAc Database (25). Gene ontology assessments were made using Webgestalt, and protein-protein interactions networks were determined using String.

Immunofluorescence staining: Ishikawa cells grown on coverslips were fixed (-20°C MeOH, 5 min) and incubated in the absence or presence of primary antibody (rabbit anti-human pMLC2; #3671, Cell Signalling Technology, mouse anti-human ZO-1; #610966, BD Biosciences, respectively or as controls (Supplementary Figure 1A), mouse anti-human KLH (Abcam UK, #ab67682), which is an irrelevant antigen, mouse serum IgG or rabbit serum IgG) in PBS overnight. After washing in PBS, cells were incubated with PBS containing Alexa 488-donkey anti-rabbit IgG or Alexa 647-donkey anti-mouse IgG antibody (both Life Technologies, Inchinnan, UK; #A-21206 and #A-31571, respectively) and DAPI (Sigma) for 1h before mounting on glass slides using Mowiol 4-88 mounting medium (Sigma) containing 3% 1,4-diazabicyclo[2.2.2]octane (Sigma). Cells and immune complexes were visualised using a Zeiss Axiophot microscope equipped with an Apotome module for optical sectioning. Images were analysed and processed using Zeiss Zen software and ImageJ. Fluorescence intensity was analysed using a Kruskal-Wallis test with Dunn's multiple comparisons post-hoc test.

Ishikawa 3D cultures and spheroid lumen analysis: Single cell suspensions of Ishikawa cells seeded at low density in drops of growth factor-reduced Matrigel (Corning) were cultured in 5mM glucose or 17mM glucose in the absence or presence of either 100µM DON or 10µM OSMI1 for 6 days then fixed (4% paraformaldehyde), quenched (50mM ammonium

chloride) and permeabilised (0.5% Triton-X100) before staining, as described above, for actin (Alexa Fluor 568 phalloidin; Life Technologies) and nuclei (DAPI). Optical sections were obtained at 0.24μm increments and images processed and assessed using Zeiss Zen software and image J to determine the number of 3D structures with a single lumen as a percentage of the total number of 3D structures. Data were analysed using a Kruskal-Wallis test with Dunn's multiple comparisons post-hoc test.

Immunoprecipitation and western blotting: Lysates from Ishikawa cells cultured in 5mM glucose or 17mM glucose in the absence or presence of 10μM OSMI1 were immunoprecipitated for myosin phosphatase target subunit 1 (MYPT1) using an anti-MYPT1 antibody (1μg, Invitrogen, #PA5-87459; 2h at 4C) and protein G-conjugated agarose beads (Pierce; 1h at 4C). Washed beads were eluted into Laemelli sample buffer and proteins separated by 10% acrylamide SDS PAGE, then transferred onto nitrocellulose membranes. After blocking in 4% BSA, membranes were incubated (2h at room temperature) with an anti-O-GlcNAc antibody (CTD; Sigma, UK; #O7764) or anti-MYPT1 antibody (Invitrogen) followed by secondary antibodies (IRDye, LI-COR Biosciences) for 1h and analysis using the Li-COR Odyssey infrared imaging system.

Analysis of global protein O-GlcNAcylation levels by dot blotting: Ishikawa cells were grown to confluence in 5mM glucose then switched to fresh 5mM glucose media for 24h or to 17mM glucose media for 24h. Cells were lysed in RIPA buffer (Sigma) supplemented with protease inhibitors (Sigma), phosphatase inhibitors (Sigma) and OSMI and Thiamet-g (10μM and 5μM respectively). 2μg protein from each sample was dotted onto nitrocellulose membranes, which were air dried, blocked with 4% BSA and washed with PBS 0.1% tween before incubating with mouse anti-OGlcNAc (CTD; Sigma) or rabbit anti-Actin (Proteintech; #20536-1-AP) antibodies (2h at room temperature with agitation). After incubation with secondary antibodies (1h RT with agitation; donkey anti-mouse IRDye 680; #926-68072 and donkey anti-rabbit IRDye 800; #926-32213). Membranes were analysed using the Li-COR Odyssey infrared imaging system and Image J software.

Results

Glucose regulates Ishikawa cell receptivity to embryos through protein O-GlcNAcylation

In vitro implantation studies, including those from our own laboratory (22), typically use standard cell culture medium, which contains supra-physiological glucose levels (17mM). Here we show that the stable attachment of blastocysts to endometrial epithelial (Ishikawa)

cells, which occurs between E5.5 and E6.5 in this model (22), was markedly reduced at physiologically relevant glucose levels (5mM; Figure 1A). Supplementing medium with estrogen and progesterone to mimic the late secretory phase had no effect on receptivity at 5mM glucose (data not shown) in keeping with our previous findings in 17mM glucose (22). Culturing cells in 5mM glucose prior to switching to 17mM glucose at the onset of co-culture with E5.5 embryos led to significantly reduced blastocyst attachment, whilst growth in 17mM glucose before switching to 5mM glucose did not affect initial attachment but significantly reduced attachment levels after 12h (Figure 1B). This suggests that glucose-induced changes to epithelial function, rather than blastocyst-attachment potential, underpin these observations. Although glucose did not alter global protein O-GlcNAcylation levels (Supplementary Figure 1B), exposure of Ishikawa cells cultured in 17mM glucose to inhibitors of GFPT1 (DON) or OGT (OSMI), key enzymes in the HBP, suggested that glucose mediates its effects on epithelial cell function via changes to protein O-GlcNAcylation, as the rate of blastocyst attachment was slower and similar to that observed in cells cultured in 5mM glucose (Figure 1C). Preventing de-O-GlcNAcylation in 5mM glucose conditions, by inhibiting the activity of OGA using Thiamet-g, did not accelerate blastocyst attachment Figure 1C). Together, these data suggest that glucose-induced, but not aberrant maintenance of, specific protein O-GlcNAcylation events stimulates receptivity to blastocyst attachment in Ishikawa cells.

Previously we showed that, pre-attachment, blastocyst-epithelial interactions regulate trophectoderm genes required for post-attachment invasion (22). We next asked whether this embryonic response is influenced by the glucose level to which the epithelial cells have been exposed. Comparison of blastocysts cultured at 5mM glucose in the absence or presence of Ishikawa cells during E4.5-E5.5 revealed that only the latter exhibited reduced attachment when switched to 17mM glucose for co-culture from E5.5-6.5 (Figure 2A). This effect was caused by embryo contact with non-receptive Ishikawa cells, as embryos that were co-cultured at 5mM glucose in permeable transwells suspended above the epithelial layer were able to attach when subsequently transferred to receptive Ishikawa cells (17mM glucose; Figure 2B). Interestingly, there was a trend for reduced expression of the trophectoderm genes *Hand1* and *Eomes*, which are known to be regulated during blastocyst implantation (22, 26) in blastocysts directly co-cultured with Ishikawa cells at 5mM glucose (Figure 2C).

Glucose regulates Ishikawa cell receptivity to embryos through protein O-GlcNAcylation-mediated changes to epithelial polarity

Previous work in breast cancer cells has demonstrated that alterations to epithelial function in response to glucose-induced protein O-GlcNAcylation include changes to cellular polarity

(27). As a reduction in polarity is a recognised feature of receptive endometrium (28), we investigated the effect of glucose, and HBP inhibitors, on Ishikawa cell polarity by determining their ability to form organised structures when grown in 3D culture.

In 5mM glucose, formation of gland-like structures with a single lumen (Figure 3A) was frequently observed (Figure 3B). At 17mM glucose, such structures were much less common, and instead, the spheroids were more likely to contain multiple, closely apposed lumens (Figure 3A, B). Importantly, the ability of cells to form properly organised (single lumen) structures in the presence of high glucose levels was increased when protein O-GlcNAcylation was inhibited by the addition of either DON or OSMI (Figure 3B), consistent with a role for this modification in glucose-mediated reduction of epithelial polarisation.

Identifying endometrial proteins O-GlcNAcylated in response to glucose

Ishikawa cell proteins with affinity for the O-GlcNAc-binding lectin, sWGA (Supplementary Figure 1C), were analysed by mass spectroscopy to characterise glucose-induced changes to the O-GlcNAcome (Supplementary file 1). Hierarchical clustering analysis (Figure 4A) of the proteins differentially present in cells cultured with 17mM versus 5mM glucose (Supplementary Figure 2A) or the OGT inhibitor OSMI (Supplementary Figure 2B) revealed 32 proteins broadly exhibiting glucose-responsive, OSMI-sensitive enrichment (Figure 4A). Some of these are already known to be O-GlcNAcylated, many on multiple sites (Figure 4B) (25). A second OSMI-sensitive cluster also contained proteins with multiple mapped O-GlcNAc sites, and though these were not enriched in response to glucose (Figure 4A, B), the observation that the most abundant proteins within these clusters (Supplementary Figure 2C) tend to have the most mapped O-GlcNAc sites validates the use of OSMI as a tool for identifying O-GlcNAcylated proteins from sWGA-binding fractions.

Analysis of the full proteome of Ishikawa cells exposed to 5mM or 17mM glucose in the absence / presence of OSMI (Supplementary file 1) demonstrated differential expression of 92 proteins associated with various biological processes (Supplementary Figure 3A-C; Supplementary Tables 1 and 2). Only three of these proteins, (HSPA4, ATP2A2 and CCT2), were amongst the 96 distinct proteins enriched in the O-GlcNAcomes, suggesting that differential sWGA enrichment reflects changes in O-GlcNAcylation rather than protein expression. Protein-protein interaction analysis of the glucose-responsive, OSMI-sensitive O-GlcNAcome cluster identified four high-confidence protein networks of RNA-binding, mitochondrial and nuclear proteins, and a network of three proteins, PPP1R12A, RHOA and RAP1B, in the Rho GTPase pathway that influences epithelial polarity (Figure 4C).

Glucose / O-GlcNAcylation regulates epithelial polarity and Ishikawa cell receptivity through the Rho GTPase pathway

Our data suggest that PPP1R12A, also known as MYPT1, is the likely O-GlcNAcylation-regulated node within the network as it is reported to be highly O-GlcNAcylated [37] and was enriched in high abundance (Figure 4B, Supplementary Figure 3), whereas RHOA and RAP1B are not predicted to harbour strong O-GlcNAcylation sites (25). MYPT1, confirmed by immunoprecipitation and western blotting to be O-GlcNAcylated in a glucose- and OSMI-sensitive manner (Figure 4D; Supplementary Figure 4), acts as the myosin-targeting subunit of protein phosphatase 1 to de-activate myosin II. We therefore investigated whether glucose-regulated changes in O-GlcNAcylation could influence epithelial polarity via myosin activity.

In polarised epithelial cells, the active (phosphorylated) form of myosin II light chain (pMLC2) localises near zona occludins (ZO)-1-positive apical tight junctions (29). Initial experiments confirmed that Ishikawa cells cultured in 5mM glucose conform to this paradigm (Figure 5A). Strikingly, and in keeping with the hypothesis that high glucose levels disrupt Ishikawa cell polarity, culture at 17mM glucose effectively abolished pMLC2 localisation near the apicolateral boundary, whereas inclusion of OSMI1 to inhibit glucose-stimulated O-GlcNAcylation prevented loss of apical pMLC2 (Figure 5A). Next, in the absence of an available specific inhibitor of MYPT1, we sought corroboratory evidence for its role in regulating myosin-II function in epithelial polarity by examining the effect of disrupting the activity of enzymes up- and downstream of MYPT1. Inhibiting Rho-activated kinase (ROCK) with Y27632, thereby preventing the phosphorylation and de-activation of MYPT1, mimics the effects of glucose on Ishikawa cells by preventing apical localisation of pMLC2 (Figure 5B) and inhibiting epithelial polarity in 3D culture (Figure 5C). Directly inhibiting myosin II with Blebbistatin has a similar effect (Figure 5B,C). Importantly, the changes to polarity induced by the inhibition of myosin improved the receptivity of Ishikawa cells cultured in 5mM glucose, as blastocysts now attached at a similar rate to those co-cultured with cells in 17mM glucose (Figure 5D). Together these data suggest that O-GlcNAcylation of MYPT1 in high glucose conditions leads to de-activation of myosin II at apical junctions and reduced epithelial polarity.

Discussion

Here we investigated the effects of glucose and glucose-responsive protein O-GlcNAcylation on endometrial function at the onset of pregnancy. We acknowledge the limitations of using an *in vitro* model that combines mouse embryos with human carcinoma-derived endometrial epithelial cells as the responses, and underlying molecular mechanisms, may not faithfully recapitulate the *in vivo* situation. Nonetheless, our data suggest that glucose may regulate endometrial receptivity and that high levels promote blastocyst attachment by means of a subtle reduction in epithelial cell polarity. Our findings are in keeping with a previous report

of decreased trophoblast spheroid adhesion to endometrial epithelial cells in which capacity for glucose uptake had been reduced by silencing of *GLUT1* (30). Other studies, using endometrial epithelial cell lines with varying degrees of polarity, have shown this parameter to influence trophoblast attachment (31) and invasion (32), however the potential for glucose to affect the critical gateway to pregnancy initiation by activating molecular pathways that control actomyosin contractility is novel. The notion that glucose can regulate polarity is supported by observations of human breast cells, as non-malignant cells lose integrity when their capacity for glucose uptake is increased via overexpression of GLUT3 (27), whereas polarity of malignant cells is restored by culture in low glucose. Importantly, loss of polarity depends on the HBP and activity of OGT (27), in line with our demonstration of phenotypic reversal when cells cultured in high glucose were exposed to inhibitors of the HBP (DON) or OGT (OSMI).

Interestingly, endometrial expression of *OGT* is higher in the secretory compared to the proliferative phase of the menstrual cycle, which correlates with the higher level of O-GlcNAcylated proteins observed, mainly in luminal and glandular epithelial cells, during this phase (33). Moreover, expression of the O-GlcNAc cycling enzymes differs between endometrial epithelial cells with differing receptivity; OGT, and therefore capacity for protein O-GlcNAcylation, is increased in receptive (RL95-2) cells and OGA predominates in non-receptive (HEC-1A) cells. Indeed, consistent with the hypothesis that protein O-GlcNAcylation facilitates the early stages of implantation, trophoblast spheroids adhere better to RL95-2 cells than to HEC-1A cells, but the finding is reversed following silencing of *OGT* or *OGA* in the respective cell lines (33). In our study of Ishikawa cells, high glucose levels induced changes to the O-GlcNAcylation status of specific proteins rather than elevating protein O-GlcNAcylation *per se* and therefore it is not surprising that receptivity was not enhanced by preventing (with Thiamet-g) de-GlcNAcylation of proteins modified in 5mM glucose. O-GlcNAcylation of the proteins identified in the current study, particularly MYPT1, could underlie the correlation between OGT activity and receptivity observed in other endometrial epithelial cell lines. However, studies in organoid models that are not cancer-derived (34) are needed to fully explore the mechanisms behind glucose-regulated receptivity.

Epithelial polarity is largely organised by the cytoskeleton working in conjunction with junctional proteins that are assembled and maintained in adhesion complexes by tension applied through active myosin II-stimulated contraction of the actomyosin network (29). Here we observed loss of active myosin-II from junctional complexes when cells were cultured in high glucose, which would facilitate the reduction in tension required for changes in polarity. Activity of myosin II is regulated by myosin light chain kinase, which is activated by ROCK-mediated phosphorylation in tight barrier epithelia (35). Hence polarity of Ishikawa cells was

406 reduced following inhibition of ROCK activity. However myosin II activity is also controlled by
407 changes to the phosphorylation status of MYPT1, the regulatory subunit of myosin light
408 chain phosphatase (MLCP) (36). ROCK-induced phosphorylation of MYPT1 blocks the
409 active site of PP1C, the catalytic subunit of MLCP, thereby facilitating maintenance of
410 myosin II activity. Previous work in fibroblasts has demonstrated that MYPT1 function is
411 regulated by glucose-dependent O-GlcNAcylation, as O-GlcNAc modification of Ser/Thr
412 sites, important for MYPT1-ROCK binding, prevents MYPT1 phosphorylation and ultimately
413 actin contractility (37). Our finding of increased O-GlcNAcylation of MYPT1 in cultures
414 exposed to high glucose points to a reduction in MYPT1 phosphorylation and therefore
415 enhanced MLCP activity that could lead to de-phosphorylation of myosin II (Figure 6). We
416 propose that such inactivation of apical junction myosin II, and the consequential reduction in
417 epithelial cytoskeletal contractility, produces a phenotype in endometrial epithelial cells that
418 is receptive to blastocyst trophectoderm attachment (Figure 6).
419 Our previous work using this in vitro model shows that trophectoderm/trophoblast lineage
420 specification factors are responsive to signals from the maternal epithelium (22) and others
421 have shown that trophectoderm sensitivity to altered environments can affect later placental
422 growth (38). Recently, we reported that a global increase of O-GlcNAcylation achieved by
423 inhibition of OGA leads to downregulation of genes associated with the TE (pre-implantation)
424 phenotype (23). While this may lead to enhanced trophoblast differentiation and increased
425 invasion at implantation (23), it could also have detrimental effects on placental cell
426 population size and homeostasis later in pregnancy (39). Here we report apparent changes
427 in trophoblast gene expression mediated by glucose-sensitive, O-GlcNAcylation-dependent
428 contact with endometrial epithelial cells, which suggests that protein O-GlcNAcylation
429 regulates the signals presented to embryos by endometrial epithelial cells at implantation.
430 Consequently, in women with diabetes, implantation in the presence of chronically or
431 intermittently high glucose levels could disrupt early trophoblast development, leading to
432 altered placental morphology and function, with negative effects on fetal growth and adult
433 health. Identification of these early signals is a priority for further research.
434 Endometrial cells cannot synthesise glucose de *novo* and must take it up via glucose
435 transporters (GLUTs) and the sodium-glucose linked transporter, SGLT1 (40). Luminal and
436 glandular epithelial cells express GLUT1, GLUT4 and SGLT1, with peak expression of
437 insulin-dependent GLUT4 during the proliferative phase (41) and higher levels of insulin-
438 insensitive GLUT1 and SGLT1 in the secretory phase (30, 41, 42). The latter are critical for
439 early pregnancy in mice as silencing of *Glut1* and loss of *Sglt1* both lead to a reduction in the
440 number of implantation sites (30, 42). Moreover, *SGLT1* expression is lower in women with
441 recurrent pregnancy loss (42).

Breakdown of stored glycogen provides another mechanism for raising epithelial glucose levels. In human endometrium, glycogen accumulates in the epithelium during the late proliferative and early secretory phases of the menstrual cycle (43); such deposition is reduced in women with unexplained infertility (43). Peri-implantation mobilisation of glycogen stores occurs in many species (44), purportedly as a source of glucose for histotrophic support of the early embryo (44). However *in utero* inhibition of glycogen phosphorylase M (PYGM), the enzyme responsible for glycogen breakdown, detrimentally affected receptivity markers and reduced the number of both endogenous, and transferred, embryo implantation sites, suggesting that this process is also important for endometrial receptivity (45).

Together these published data add to our model of molecular mechanisms underlying glucose control of endometrial epithelial function (Figure 6) by suggesting that deposition (during the proliferative phase) and then breakdown (early secretory phase) of glycogen may be needed to provide a glucose surge that drives the HBP and O-GlcNAcylation of proteins that facilitate loss of epithelial polarity. Luteal progesterone is often reported as the key regulator of endometrial glycogen synthesis (44) though *in vitro* studies of Ishikawa and primary cells have demonstrated that insulin, rather than medroxyprogesterone acetate, stimulates both the expression and activity of glycogen synthase (46).

Some women with type 1 diabetes experience a decline in insulin sensitivity during the early secretory phase of the menstrual cycle (47) and although little is known about the existence of insulin resistance in the endometrium (48), its presence could lead to a reduction in glycogen synthesis. Furthermore, impaired insulin-regulated glucose transport and glycogen metabolism is thought to underpin the reduction in endometrial receptivity markers and number of implantation sites observed in a mouse model of type 2 diabetes (49). Consequently, in women with diabetes, endometrial epithelial flux of glucose through the HBP may be insufficient to modulate protein O-GlcNAcylation and polarity, leading to impaired implantation and reduced fecundity. Alternatively, should endometrial insulin sensitivity be maintained, temporally inappropriate activation of the HBP, and therefore changes to endometrial epithelial cell polarity, may result in a prolonged receptivity window, permitting implantation of developmentally incompetent embryos and a pregnancy that ultimately ends in miscarriage. Both increased time to pregnancy, and the incidence of spontaneous abortion, are prevalent in women with diabetes (4, 50). Experiments to determine the activity of glucose/glycogen processing enzymes, the HBP and phosphorylation/localisation of myosin II in endometrial epithelial cell organoids which, in other conditions, retain their phenotype (51), derived from women with diabetes, will be useful for establishing the veracity of our proposed model.

In summary, we have shown that glucose influences endometrial receptivity and identified O-GlcNAcylation of proteins that regulate epithelial polarity and the localisation of tight junction

proteins required for embryo attachment as a molecular switch linking glucose metabolism with early pregnancy success/failure.

Supplemental Material: Supplementary Figures S1-S4 and Supplementary Tables 1 and 2 are available at: https://doi.org/10.48420/24306505

Data availability: The O-GlcNAcome and proteome datasets generated and analysed during the current study are available at https://doi.org/10.48420/24306481.v1

Acknowledgements: Mass spectrometry was conducted by the University of Manchester Biological Mass Spectrometry core facility (RRID code SCR_020987).

Funding: This work was funded through a Diabetes UK project grant (15/0005207).

Competing Interests: The authors have no relevant financial or non-financial interests to disclose.

Author Contributions: MW, JDA, DRB, SJK and JJB conceptualised the study and secured funding, with input from PTR. MW, JDA, DRB, SJK and JJB supervised all parts of the study. PTR, IP, BR, SCB, LR and DA performed the experiments. PTR, JDA, DRB, SJK, JJB and MW analysed and interpreted data. PTR and MW wrote the manuscript with input from all authors.

Ethics approval: All procedures involving animals were licensed under the authority of a UK Home Office project license (PPL 70/07838) and were authorised by the Animal Welfare and Ethical Review Board of the University of Manchester, according to the Animal Act, 1986.

References

1. **Wild S, Roglic G, Green A, Sicree R, and King H**. Global prevalence of diabetes: estimates for the year 2000 and projections for 2030. *Diabetes Care* 27: 1047-1053, 2004.
2. **Mackin ST, Nelson SM, Kerssens JJ, Wood R, Wild S, Colhoun HM, Leese GP, Philip S, Lindsay RS, and Group SE**. Diabetes and pregnancy: national trends over a 15 year period. *Diabetologia* 61: 1081-1088, 2018.
3. **Greene MF**. Spontaneous abortions and major malformations in women with diabetes mellitus. *Semin Reprod Endocrinol* 17: 127-136, 1999.
4. **Bell R, Bailey K, Cresswell T, Hawthorne G, Critchley J, and Lewis-Barned N**. Trends in prevalence and outcomes of pregnancy in women with pre-existing type I and type II diabetes. *BJOG* 115: 445-452, 2008.

5. **American Diabetes A**. 13. Management of Diabetes in Pregnancy: Standards of Medical Care in Diabetes-2018. *Diabetes Care* 41: S137-S143, 2018.
6. **Murphy HR, Bell R, Cartwright C, Curnow P, Maresh M, Morgan M, Sylvester C, Young B, and Lewis-Barned N**. Improved pregnancy outcomes in women with type 1 and type 2 diabetes but substantial clinic-to-clinic variations: a prospective nationwide study. *Diabetologia* 60: 1668-1677, 2017.
7. **Kyne-Grzebalski D, Wood L, Marshall SM, and Taylor R**. Episodic hyperglycaemia in pregnant women with well-controlled Type 1 diabetes mellitus: a major potential factor underlying macrosomia. *Diabet Med* 16: 702-706, 1999.
8. **Leese HJ**. The formation and function of oviduct fluid. *J Reprod Fertil* 82: 843-856, 1988.
9. **Sinzato YK, Volpato GT, Iessi IL, Bueno A, Calderon Ide M, Rudge MV, and Damasceno DC**. Neonatally induced mild diabetes in rats and its effect on maternal, placental, and fetal parameters. *Exp Diabetes Res* 2012: 108163, 2012.
10. **Albaghdadi AJ, and Kan FW**. Endometrial receptivity defects and impaired implantation in diabetic NOD mice. *Biol Reprod* 87: 30, 2012.
11. **Aplin JD, and Ruane PT**. Embryo-epithelium interactions during implantation at a glance. *J Cell Sci* 130: 15-22, 2017.
12. **Murphy CR**. Uterine receptivity and the plasma membrane transformation. *Cell Res* 14: 259-267, 2004.
13. **Sharkey AM, and Smith SK**. The endometrium as a cause of implantation failure. *Best Pract Res Clin Obstet Gynaecol* 17: 289-307, 2003.
14. **Quenby S, Vince G, Farquharson R, and Aplin J**. Recurrent miscarriage: a defect in nature's quality control? *Hum Reprod* 17: 1959-1963, 2002.
15. **Bergh PA, and Navot D**. The impact of embryonic development and endometrial maturity on the timing of implantation. *Fertil Steril* 58: 537-542, 1992.
16. **Hart GW**. Nutrient regulation of signaling and transcription. *J Biol Chem* 294: 2211-2231, 2019.
17. **Vocadlo DJ**. O-GlcNAc processing enzymes: catalytic mechanisms, substrate specificity, and enzyme regulation. *Curr Opin Chem Biol* 16: 488-497, 2012.
18. **Wang Z, Park K, Comer F, Hsieh-Wilson LC, Saudek CD, and Hart GW**. Site-specific GlcNAcylation of human erythrocyte proteins: potential biomarker(s) for diabetes. *Diabetes* 58: 309-317, 2009.
19. **Springhorn C, Matsha TE, Erasmus RT, and Essop MF**. Exploring leukocyte O-GlcNAcylation as a novel diagnostic tool for the earlier detection of type 2 diabetes mellitus. *JClinEndocrinolMetab* 97: 4640-4649, 2012.
20. **Schelbach CJ, Robker RL, Bennett BD, Gauld AD, Thompson JG, and Kind KL**. Altered pregnancy outcomes in mice following treatment with the hyperglycaemia mimetic, glucosamine, during the periconception period. *Reprod Fertil Dev* 25: 405-416, 2013.
21. **Brown HM, Green ES, Tan TCY, Gonzalez MB, Rumbold AR, Hull ML, Norman RJ, Packer NH, Robertson SA, and Thompson JG**. Periconception onset diabetes is associated with embryopathy and fetal growth retardation, reproductive tract hyperglycosylation and impaired immune adaptation to pregnancy. *Sci Rep* 8: 2114, 2018.
22. **Ruane PT, Berneau SC, Koeck R, Watts J, Kimber SJ, Brison DR, Westwood M, and Aplin JD**. Apposition to endometrial epithelial cells activates mouse blastocysts for implantation. *Mol Hum Reprod* 23: 617-627, 2017.
23. **Ruane PT, Tan CMJ, Adlam DJ, Kimber SJ, Brison DR, Aplin JD, and Westwood M**. Protein O-GlcNAcylation Promotes Trophoblast Differentiation at Implantation. *Cells* 9: 2020.
24. **Palin V, Russell M, Graham R, Aplin JD, and Westwood M**. Altered protein O-GlcNAcylation in placentas from mothers with diabetes causes aberrant endocytosis in placental trophoblast cells. *Sci Rep* 11: 20705, 2021.
25. **Wulff-Fuentes E, Berendt RR, Massman L, Danner L, Malard F, Vora J, Kahsay R, and Olivier-Van Stichelen S**. The human O-GlcNAcome database and meta-analysis. *Sci Data* 8: 25, 2021.

26. **Awonuga AO, Zhong W, Abdallah ME, Slater JA, Zhou SC, Xie YF, Puscheck EE, and Rappolee DA**. Eomesodermin, HAND1, and CSH1 proteins are induced by cellular stress in a stress-activated protein kinase-dependent manner. *Mol Reprod Dev* 78: 519-528, 2011.
27. **Onodera Y, Nam JM, and Bissell MJ**. Increased sugar uptake promotes oncogenesis via EPAC/RAP1 and O-GlcNAc pathways. *J Clin Invest* 124: 367-384, 2014.
28. **Zhang Y, Du X, Chen X, Tang H, Zhou Q, He J, Ding Y, Wang Y, Liu X, and Geng Y**. Rictor/mTORC2 is involved in endometrial receptivity by regulating epithelial remodeling. *FASEB J* 35: e21731, 2021.
29. **Arnold TR, Stephenson RE, and Miller AL**. Rho GTPases and actomyosin: Partners in regulating epithelial cell-cell junction structure and function. *Exp Cell Res* 358: 20-30, 2017.
30. **Zhang H, Qi J, Wang Y, Sun J, Li Z, Sui L, Fan J, Liu C, Shang Y, Kong L, and Kong Y**. Progesterone Regulates Glucose Metabolism Through Glucose Transporter 1 to Promote Endometrial Receptivity. *Front Physiol* 11: 543148, 2020.
31. **Peng J, Li X, Zhang Y, Hu J, Shang Y, Yin Y, and Xiao Z**. Par3/integrin beta1 regulates embryo adhesion via changing endometrial luminal epithelium polaritydagger. *Biol Reprod* 104: 1228-1238, 2021.
32. **Buck VU, Gellersen B, Leube RE, and Classen-Linke I**. Interaction of human trophoblast cells with gland-like endometrial spheroids: a model system for trophoblast invasion. *Hum Reprod* 30: 906-916, 2015.
33. **Han X, Li X, Liu H, Zhang H, Li A, Dong M, Xu Y, Yan B, Sui L, and Kong Y**. OGlcNAc modification influences endometrial receptivity by promoting endometrial cell proliferation, migration and invasion. *Oncol Rep* 42: 2065-2074, 2019.
34. **Turco MY, Gardner L, Hughes J, Cindrova-Davies T, Gomez MJ, Farrell L, Hollinshead M, Marsh SGE, Brosens JJ, Critchley HO, Simons BD, Hemberger M, Koo BK, Moffett A, and Burton GJ**. Long-term, hormone-responsive organoid cultures of human endometrium in a chemically defined medium. *Nat Cell Biol* 19: 568-577, 2017.
35. **Szaszi K, Sirokmany G, Di Ciano-Oliveira C, Rotstein OD, and Kapus A**. Depolarization induces Rho-Rho kinase-mediated myosin light chain phosphorylation in kidney tubular cells. *Am J Physiol Cell Physiol* 289: C673-685, 2005.
36. **Kiss A, Erdodi F, and Lontay B**. Myosin phosphatase: Unexpected functions of a long-known enzyme. *Biochim Biophys Acta Mol Cell Res* 1866: 2-15, 2019.
37. **Pedowitz NJ, Batt AR, Darabedian N, and Pratt MR**. MYPT1 O-GlcNAc modification regulates sphingosine-1-phosphate mediated contraction. *Nat Chem Biol* 17: 169-177, 2021.
38. **de Waal E, Vrooman LA, Fischer E, Ord T, Mainigi MA, Coutifaris C, Schultz RM, and Bartolomei MS**. The cumulative effect of assisted reproduction procedures on placental development and epigenetic perturbations in a mouse model. *Hum Mol Genet* 24: 6975-6985, 2015.
39. **Yang Y, Bolnick A, Shamir A, Abdulhasan M, Li Q, Parker GC, Puscheck EE, and Rappolee DA**. Blastocyst-Derived Stem Cell Populations under Stress: Impact of Nutrition and Metabolism on Stem Cell Potency Loss and Miscarriage. *Stem Cell Rev Rep* 13: 454-464, 2017.
40. **Vrhovac Madunic I, Karin-Kujundzic V, Madunic J, Sola IM, and Serman L**. Endometrial Glucose Transporters in Health and Disease. *Front Cell Dev Biol* 9: 703671, 2021.
41. **Mioni R, Mozzanega B, Granzotto M, Pierobon A, Zuliani L, Maffei P, Blandamura S, Grassi S, Sicolo N, and Vettor R**. Insulin receptor and glucose transporters mRNA expression throughout the menstrual cycle in human endometrium: a physiological and cyclical condition of tissue insulin resistance. *Gynecol Endocrinol* 28: 1014-1018, 2012.
42. **Salker MS, Singh Y, Zeng N, Chen H, Zhang S, Umbach AT, Fakhri H, Kohlhofer U, Quintanilla-Martinez L, Durairaj RRP, Barros FSV, Vrljicak P, Ott S, Brucker SY, Wallwiener D, Vrhovac Madunic I, Breljak D, Sabolic I, Koepsell H, Brosens JJ, and**

Lang F. Loss of Endometrial Sodium Glucose Cotransporter SGLT1 is Detrimental to Embryo Survival and Fetal Growth in Pregnancy. *Sci Rep* 7: 12612, 2017.
43. **Maeyama M, Sudo I, Saito K, Matsuo I, and Nakahara K**. Glycogen estimation by a rapid enzymic method in very small samples of human endometrium: glycogen content in the endometrium of infertile patients during the menstrual cycle. *Fertil Steril* 28: 159-162, 1977.
44. **Dean M**. Glycogen in the uterus and fallopian tubes is an important source of glucose during early pregnancydagger. *Biol Reprod* 101: 297-305, 2019.
45. **Nie L, Zhang LX, Wang YC, Long Y, Ma YD, Liao LC, Dai XH, Cui ZH, Liu H, Wang ZQ, Ma ZY, Yuan DZ, and Yue LM**. Consistency and synchronization of AMPK-glycogen in endometrial epithelial cells are critical to the embryo implantation. *Reproduction* 163: 293-307, 2022.
46. **Flannery CA, Choe GH, Cooke KM, Fleming AG, Radford CC, Kodaman PH, Jurczak MJ, Kibbey RG, and Taylor HS**. Insulin Regulates Glycogen Synthesis in Human Endometrial Glands Through Increased GYS2. *J Clin Endocrinol Metab* 103: 2843-2850, 2018.
47. **Widom B, Diamond MP, and Simonson DC**. Alterations in glucose metabolism during menstrual cycle in women with IDDM. *Diabetes Care* 15: 213-220, 1992.
48. **Diamanti-Kandarakis E, and Dunaif A**. Insulin resistance and the polycystic ovary syndrome revisited: an update on mechanisms and implications. *Endocr Rev* 33: 981-1030, 2012.
49. **Ma YD, Cui ZH, Zhao D, Wang YC, Zhang LX, Zhang XQ, Guo WJ, Yuan DZ, Zhang JH, Yue LM, and Nie L**. The Effects of Altered Endometrial Glucose Homeostasis on Embryo Implantation in Type 2 Diabetic Mice. *Reprod Sci* 28: 703-714, 2021.
50. **Whitworth KW, Baird DD, Stene LC, Skjaerven R, and Longnecker MP**. Fecundability among women with type 1 and type 2 diabetes in the Norwegian Mother and Child Cohort Study. *Diabetologia* 54: 516-522, 2011.
51. **Boretto M, Maenhoudt N, Luo X, Hennes A, Boeckx B, Bui B, Heremans R, Perneel L, Kobayashi H, Van Zundert I, Brems H, Cox B, Ferrante M, Uji IH, Koh KP, D'Hooghe T, Vanhie A, Vergote I, Meuleman C, Tomassetti C, Lambrechts D, Vriens J, Timmerman D, and Vankelecom H**. Patient-derived organoids from endometrial disease capture clinical heterogeneity and are amenable to drug screening. *Nat Cell Biol* 21: 1041-1051, 2019.

Figure Legends

Figure 1. Glucose regulates Ishikawa cell receptivity to embryos through protein O-GlcNAcylation. (A) Ishikawa cells were grown to confluence in medium containing 5mM or 17mM glucose before addition of hatched E4.5 mouse blastocysts and culture for a further 48 hours; attachment was monitored after 28h (E5.5+4h), 32h, 36h and 48h of co-culture. **(B)** Ishikawa cells were grown in medium containing 5mm or 17mM glucose then switched to medium containing the alternative glucose concentration for 24 hours of co-culture with hatched E5.5 mouse blastocysts. **(C)** Ishikawa cells were grown in 5mm glucose ± 5μM Thiamet-g (TMG; inhibitor of OGA) or 17mM glucose in the absence or presence of either DON (100μM) or OSMI1 (10μM), inhibitors of the enzymes GFPT1 and OGT respectively, for 24 hours. All cultures were switched to medium containing only 17mM glucose (no inhibitors) before adding hatched E5.5 mouse blastocysts for 24h of co-culture. Attachment was scored after 4, 8 12 and 24 hours and data from 5 independent experiments, each using

12 blastocysts per condition, are shown as mean (±SEM) percentage of stably attached blastocysts at each time point. * - p<0.05, ** - p<0.01, *** - p<0.001; 2-way ANOVA.

Figure 2. Endometrial epithelial effects on blastocyst-attachment potential are regulated by glucose. (A) E4.5 mouse blastocysts were either co-cultured with Ishikawa cells in 5mM (-) or 17mM (-) glucose for 24 (to E5.5), then switched to 17mM glucose for a further 24h (to E6.5), or cultured alone in 5mM glucose (-) for 24h (from E4.5 to E5.5) before co-culture with Ishikawa cells in 17mM glucose for 24h (to E6.5). Stable attachment was scored from E5.5+4h. Mean ± SEM from 3 independent experiments using 12 blastocysts per condition. *p<0.05, ***p<0.001; ANOVA. **(B)** E4.5 blastocysts were co-cultured separated from Ishikawa cells with a permeable transwell in medium containing 5mMor 17mM glucose for 24h (to E5.5), then transferred to direct co-culture with Ishikawa cells at 17mM glucose for a further 24h (to E6.5). Stable attachment was scored from E5.5+4h. Mean ± SEM from 3 independent experiments using 10-12 blastocysts per condition. **(C)** E4.5 blastocysts were cultured alone in medium containing 17mM glucose, or co-cultured with Ishikawa cells in serum-free medium containing 5mM or 17mM glucose, for 24h, to E5.5. Blastocysts were lysed and RNA collected for qPCR analysis to assess the expression of Hand1 and Eomes. Fold change in expression, calculated using the 2-ΔΔct method, is presented relative to that determined in blastocysts cultured from E4.5-E5.5 in 17mM glucose without Ishikawa cells. Line represents median from at least 3 independent experiments using 10 blastocysts per condition; expression in blastocysts co-cultured with Ishikawa cells in 5mM versus 17mM glucose statistically analysed using Mann-Whitney test.

Figure 3. Glucose affects Ishikawa cell polarity via protein O-GlcNAcylation. (A) Morphology of Ishikawa cells grown in 3D culture. Cells were stained for actin (Alexa Fluor 568 phalloidin; red) and nuclei (DAPI, blue). Scale bars represent 20μm. **(B)** Ishikawa cells grown in 3D culture with 5mM glucose (n=6), 17mM glucose (n=6) or 17mM glucose + 10μM OSMI1 or 100μM DON (n=3) were stained with phalloidin and DAPI and the percentage of structures with a single lumen calculated. Line represents median. * - <0.05, ** - <0.01; Kruskal-Wallis with Dunn's multiple comparisons post hoc test.

Figure 4. Identifying proteins O-GlcNAcylated in response to glucose. Ishikawa cells (n=3) were cultured in medium containing 5mM glucose, 17mM glucose or 17mM glucose + 10μM OSMI1 then lysed and incubated with sWGA beads to enrich for O-GlcNAcylated proteins. **(A)** Isolated proteins were profiled using mass spectrometry and differentially enriched proteins (log_2 fold change) analysed using hierarchical clustering. **(B)** Known O-GlcNAcylation sites within the differentially enriched proteins were mapped using

712 www.oglcnac.mcw.edu (25). **(C)** Protein-protein interaction analysis of proteins differentially
713 enriched in a glucose-responsive, OSMI-sensitive manner (highlighted by black box in A and
714 B) identified four high confidence (FDR = 0.012) protein networks. **(D)** Lysates (input) from
715 Ishikawa cells cultured in 5mM glucose, 17mM glucose or 17mM glucose + 10μM OSMI1
716 were immunoprecipitated for MYPT1 and then precipitate, supernatant and input were
717 blotted for O-GlcNAc and MYPT1 (also known as PPP1R12A). Merged image shown; see
718 Supplementary figures for individual blots.
719
720 **Figure 5. Inhibition of ROCK reduces Ishikawa cell polarity and promotes blastocyst**
721 **attachment. (A)** Ishikawa cells (n=5) cultured in 5mM glucose, 17mM glucose or 17mM
722 glucose + 10μM OSMI1 were stained for phospho-myosin light chain 2 (pMLC; green), zona
723 occludens 1 (ZO-1; red) and nuclei (DAPI; blue). **(B)** Ishikawa cells (n=5) cultured in 5mM
724 glucose in the absence or presence of 1μM Blebbistatin or 10μM Y27632 were stained for
725 pMLC (green), ZO-1 (red) and nuclei (blue). White arrows indicate the location of the inset
726 image. Scale bars represent 20μm. Graphs shows the ratio of the immunofluorescence
727 intensity of pMLC to ZO-1 with data presented as median values ± the interquartile range. * -
728 <0.05, ** - <0.01; Kruskal-Wallis with Dunn's multiple comparisons post hoc test. **(C)** Cells
729 were grown in 3D culture with 5mM glucose in the absence or presence of 1μM Blebbistatin
730 or 10μM Y27632, stained with phalloidin and DAPI and the percentage of structures with a
731 single lumen calculated. Line represents median. * - <0.05, ** - <0.01; Kruskal-Wallis with
732 Dunn's multiple comparisons post hoc test. **(D)** Ishikawa cells were grown in 5mM glucose
733 medium alone or medium containing 10μM Y27632 or 1μM Blebbistatin before adding
734 hatched E5.5 mouse blastocysts for 24h of co-culture in fresh medium containing 17mM
735 glucose. Attachment was scored after 4, 8 12 and 24 hours and data from 6 independent
736 experiments using 10-12 blastocysts per condition are shown as mean (±SEM) percentage
737 of stably attached blastocysts at each time point. * - $p<0.05$; ANOVA.
738
739 **Figure 6. Proposed model for glucose- and O-GlcNAcylation-mediated changes to**
740 **endometrial epithelial cell polarity and receptivity at implantation.** Glucose accumulated
741 in endometrial epithelial cells during the proliferative phase is stored as glycogen due to
742 insulin-stimulated glycogen synthase kinase (GSK) and glycogen synthase (GS) activity.
743 During the secretory phase, raised intracellular glucose levels, as a consequence of
744 increased glucose uptake and glycogen breakdown, stimulates flux through the hexosamine
745 biosynthetic pathway (HBP), culminating in O-GlcNAcylation (G) of MYPT1, the regulatory
746 subunit of myosin light chain phosphatase (MLCP), which prevents MYPT1 phosphorylation
747 (P) by ROCK thereby activating MLCP (dark green) activity and inactivating (by de-
748 phosphorylation) myosin II (light yellow) which permits junctional protein (purple)

749 reorganisation, loss of polarity and increased receptivity. GP – glycogen phosphatase; MLC
750 – myosin light chain; MLCK - myosin light chain kinase; OGT – O-GlcNAc transferase. Grey
751 text / symbols denote information drawn from literature; other colours represent experiments
752 / findings from the current study.
753
754
755
756
757

Figure 1

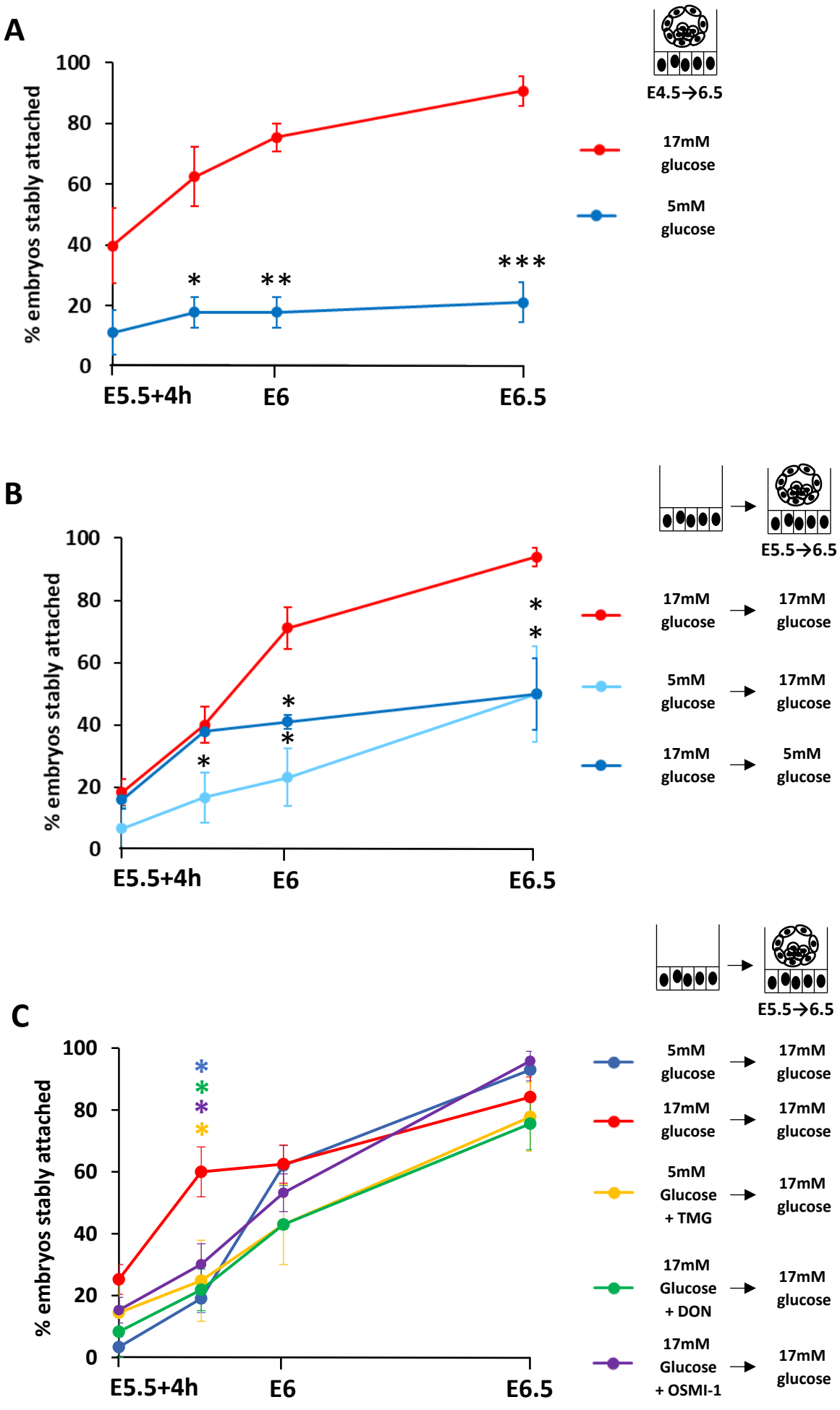
A
% embryos stably attached
100
80
60
40
20
0
E5.5+4h
E6
E6.5
*
**
***
E4.5→6.5
17mM glucose
5mM glucose
B
% embryos stably attached
E5.5→6.5
17mM glucose → 17mM glucose
5mM glucose → 17mM glucose
17mM glucose → 5mM glucose
C
% embryos stably attached
E5.5→6.5
5mM glucose → 17mM glucose
17mM glucose → 17mM glucose
5mM Glucose + TMG → 17mM glucose
17mM Glucose + DON → 17mM glucose
17mM Glucose + OSMI-1 → 17mM glucose

Figure 2

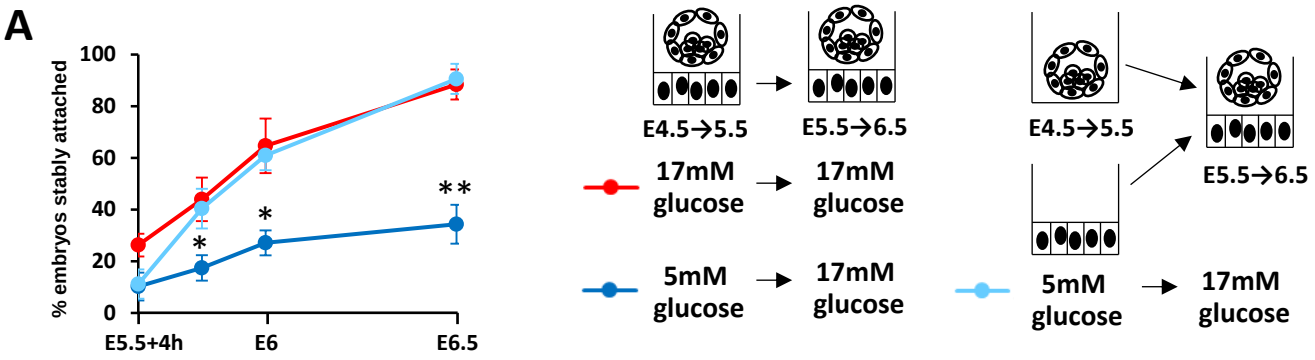
A
% embryos stably attached
100
80
60
40
20
0
E5.5+4h
E6
E6.5
*
*
**
E4.5→5.5
E5.5→6.5
17mM glucose
17mM glucose
5mM glucose
17mM glucose
E4.5→5.5
E5.5→6.5
5mM glucose
17mM glucose

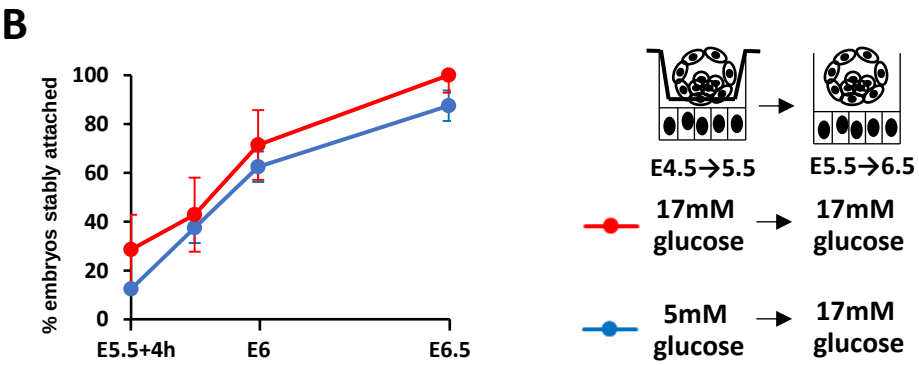
B
% embryos stably attached
100
80
60
40
20
0
E5.5+4h
E6
E6.5
E4.5→5.5
E5.5→6.5
17mM glucose
17mM glucose
5mM glucose
17mM glucose

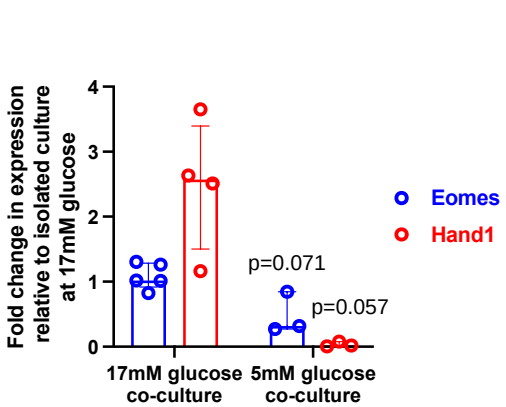
C
Fold change in expression relative to isolated culture at 17mM glucose
4
3
2
1
0
p=0.071
p=0.057
Eomes
Hand1
17mM glucose co-culture
5mM glucose co-culture

Figure 3

A

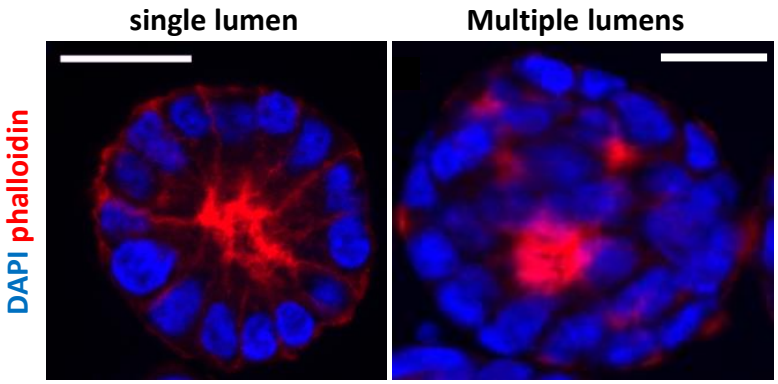
single lumen
Multiple lumens
DAPI phalloidin

B

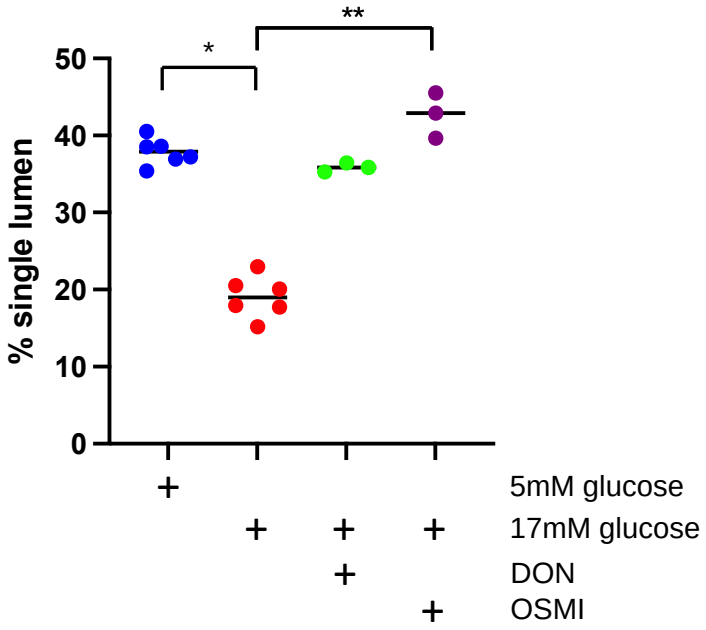
**
*
50
40
30
20
10
0
% single lumen
+
5mM glucose
+
+
+
17mM glucose
+
DON
+
OSMI

Figure 4

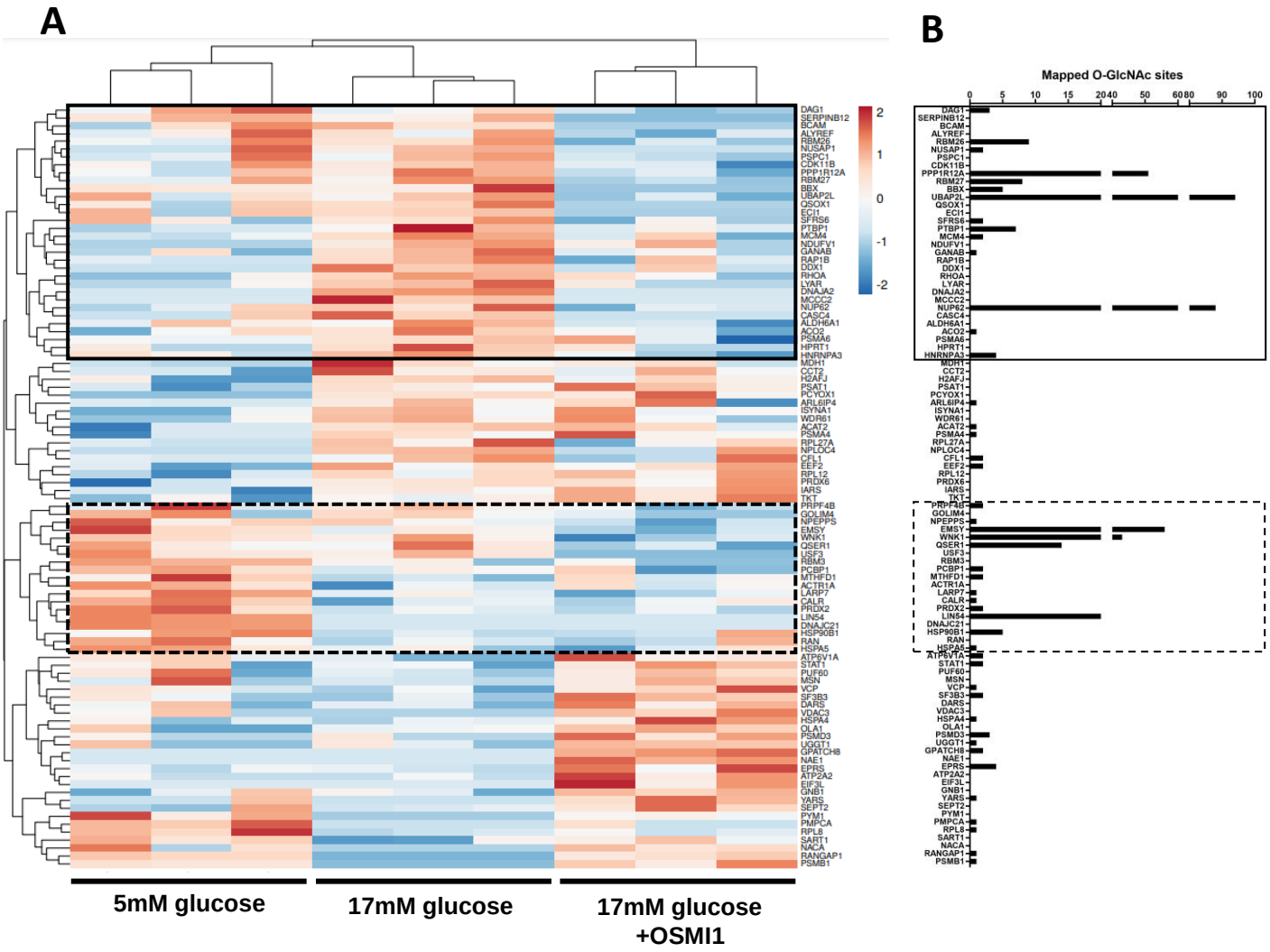
A
B
Mapped O-GlcNAc sites
5mM glucose
17mM glucose
17mM glucose +OSMI1

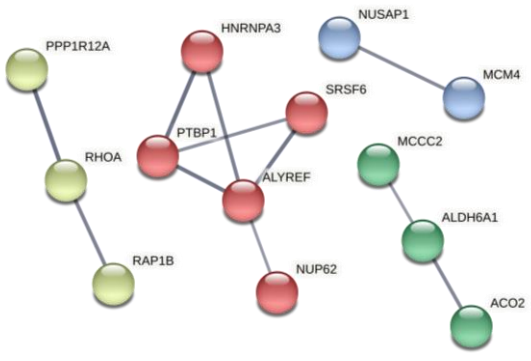
C
PPP1R12A
HNRNPA3
NUSAP1
MCM4
SRSF6
PTBP1
RHOA
ALYREF
MCCC2
ALDH6A1
RAP1B
NUP62
ACO2

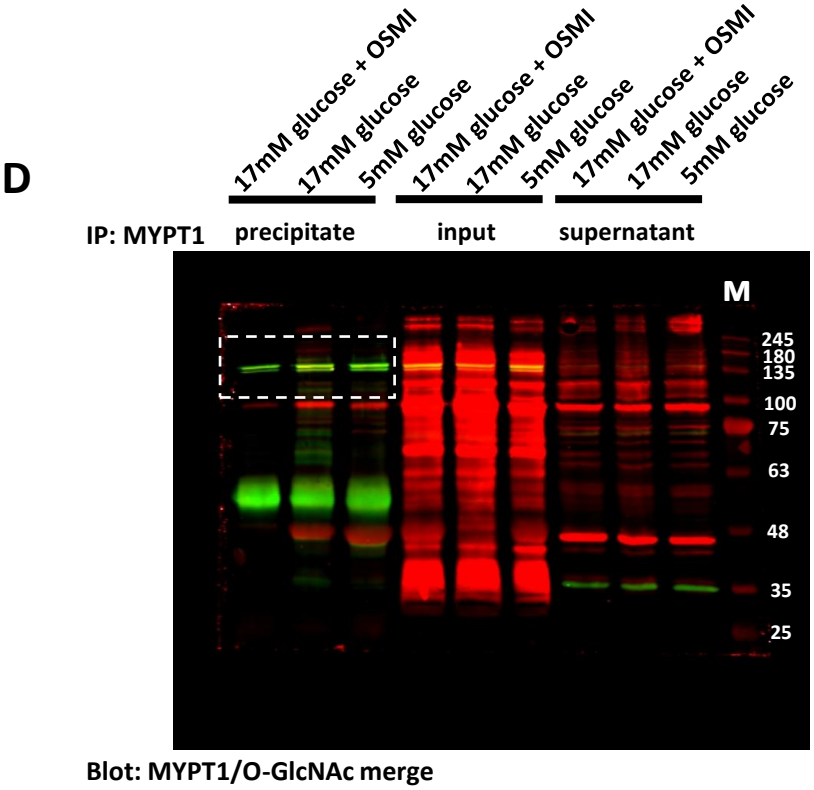
D
17mM glucose + OSMI
17mM glucose
5mM glucose
17mM glucose + OSMI
17mM glucose
5mM glucose
17mM glucose + OSMI
17mM glucose
5mM glucose
IP: MYPT1
precipitate
input
supernatant
M
245
180
135
100
75
63
48
35
25
Blot: MYPT1/O-GlcNAc merge

Figure 5

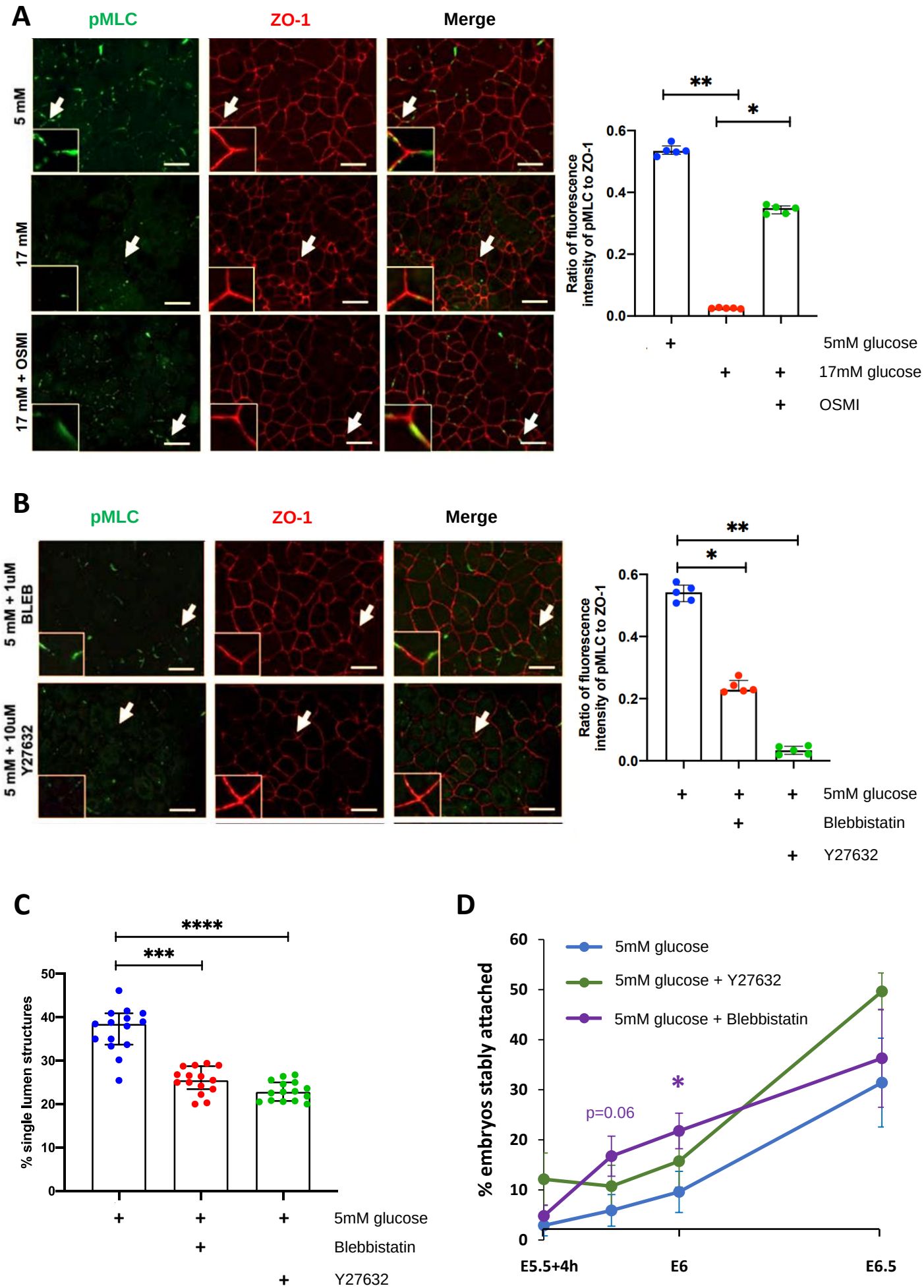
A
pMLC
ZO-1
Merge
5 mM
17 mM
17 mM + OSMI
Ratio of fluorescence intensity of pMLC to ZO-1
0.6
0.4
0.2
0.0
**
*
5mM glucose
17mM glucose
OSMI
B
pMLC
ZO-1
Merge
5 mM + 1uM BLEB
5 mM + 10uM Y27632
Ratio of fluorescence intensity of pMLC to ZO-1
0.6
0.4
0.2
0.0
**
*
5mM glucose
Blebbistatin
Y27632
C
% single lumen structures
50
40
30
20
10
0
****
***
5mM glucose
Blebbistatin
Y27632
D
% embryos stably attached
60
50
40
30
20
10
0
5mM glucose
5mM glucose + Y27632
5mM glucose + Blebbistatin
p=0.06
*
E5.5+4h
E6
E6.5

Figure 6

Proliferative phase – polarised, non-receptive endometrial epithelium

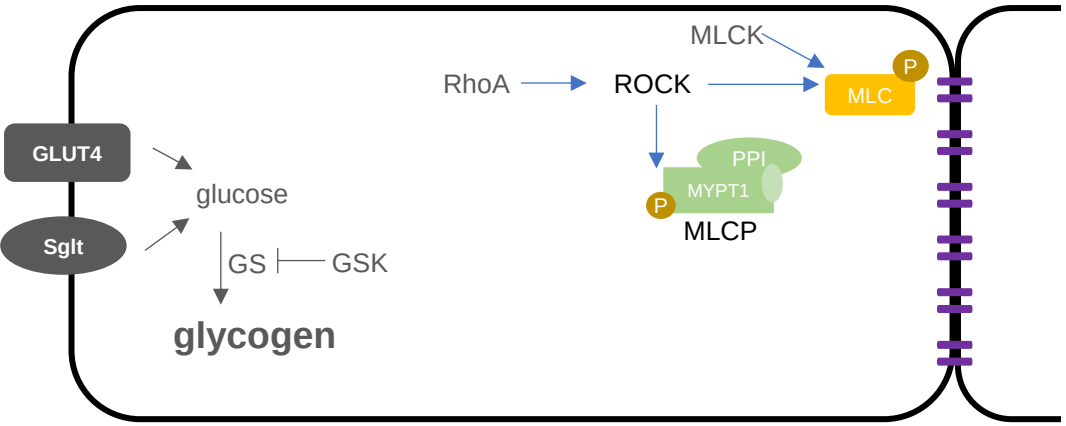

Secretory phase – partially depolarised, receptive endometrial epithelium

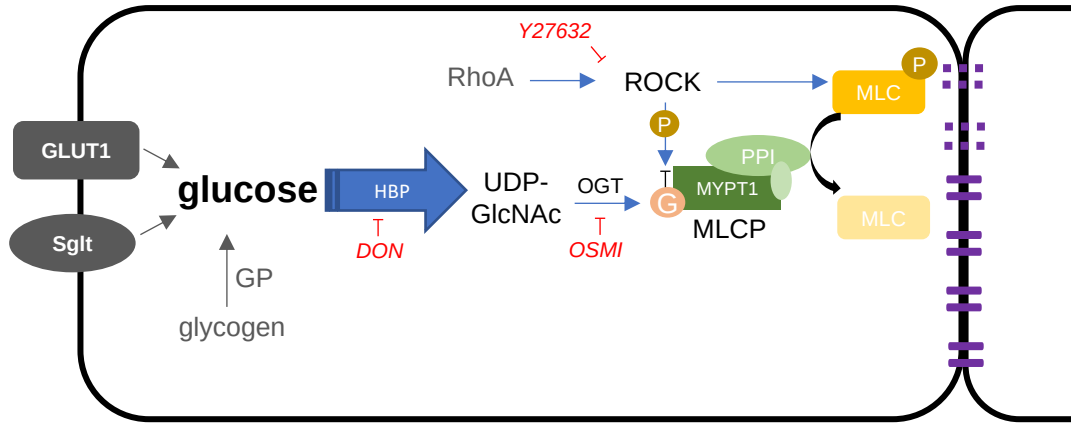

Glucose-regulated O-GlcNAcylation of proteins controlling endometrial epithelial cell polarity facilitates embryo attachment

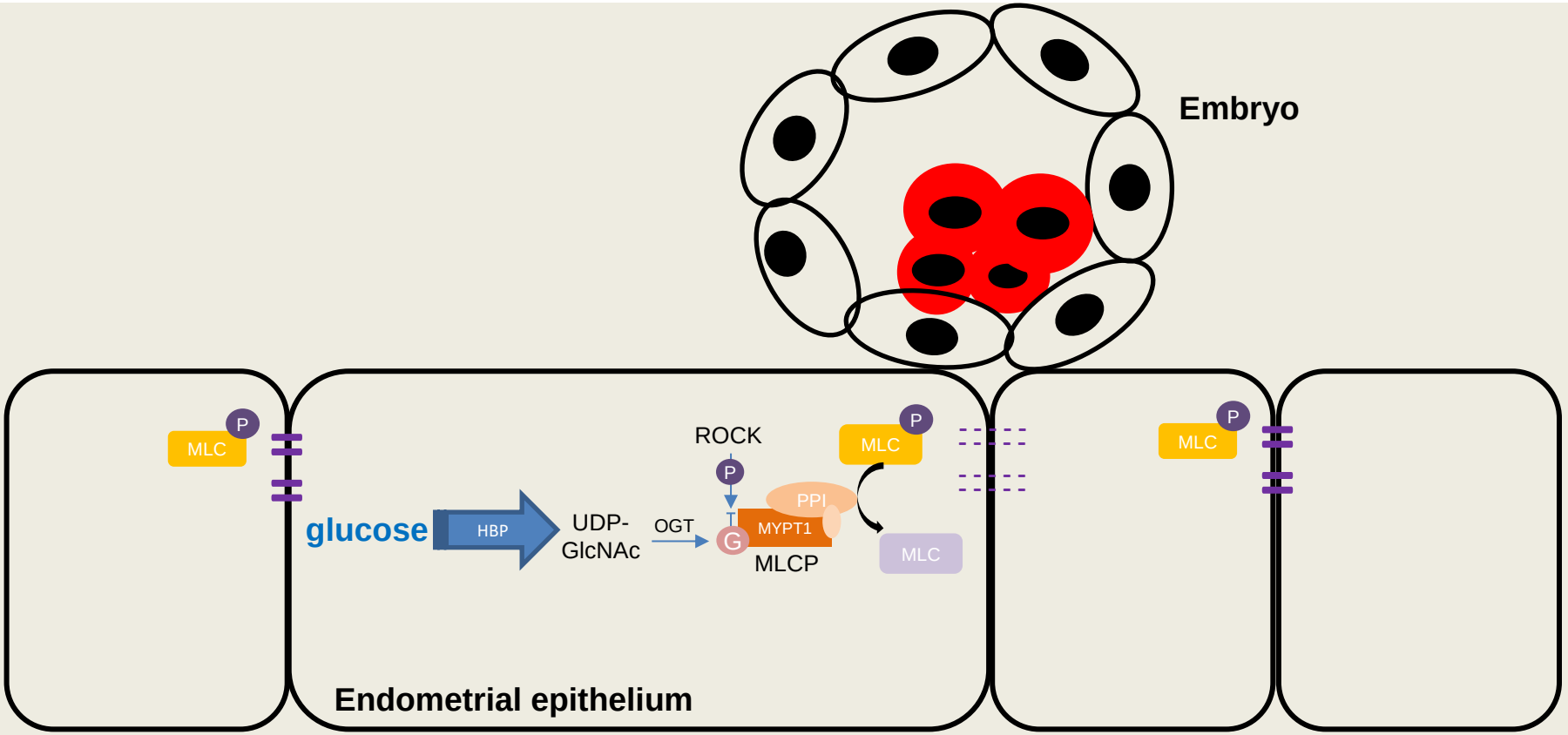

CONCLUSION: **Glucose-driven O-GlcNAcylation of MYPT1 enables MLCP de-phosphorylation of Myosin II and de-stabilisation of apical junctional complexes, leading to the reduction in endometrial epithelial polarity required for embryo attachment and subsequent implantation.**